

Supplementary information

Real-time monitoring of Trojan horse effect of silver nanoparticles by a genetically encoded fluorescent cell sensor

Fang You, Wenqin Tang, and Lin-Yue Lanry Yung*

ADDRESS: Department of Chemical and Biomolecular Engineering, National University of Singapore, 10 Kent Ridge Crescent, Singapore 119260, Singapore

*Email address: cheyly@nus.edu.sg

Additional experimental data related to UV-vis and DLS data of AgNPs in fresh DMEM medium (Figure S1), SDS-PAGE of the purified MT2a-FRET protein (Figure S2), the complete DNA and protein sequences of MT2a-FRET (Figure S3), confocal images of the MT2a-FRET cell line (Figure S4), changes of intracellular Ag concentrations in MT2a-FRET cells (Figure S5), and AgNPs dissolution in DMEM media with cell culture (Figure S6) are included in supplementary information.

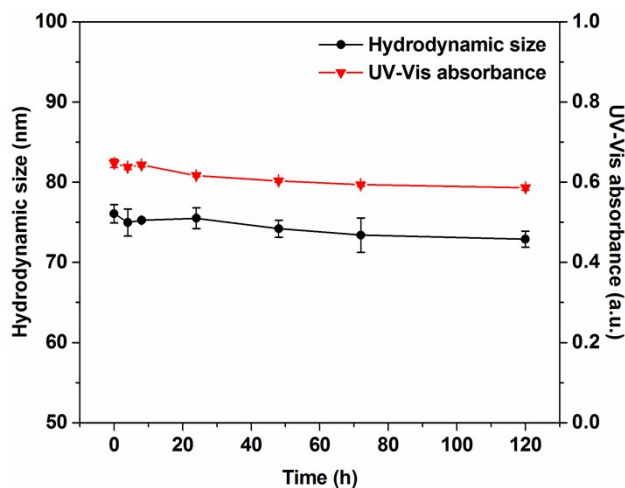


Figure S1. Stabilities of AgNPs in DMEM culture medium. UV-vis absorbance and hydrodynamic size of AgNPs in fresh DMEM medium with 10% FBS were monitored for 120h. Data are shown as mean \pm SD (n=3).

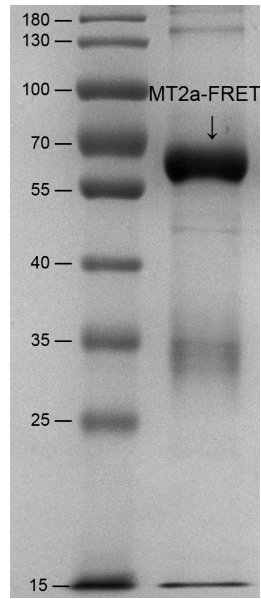


Figure S2. SDS-PAGE of the purified MT2a-FRET protein. Left lane: GeneRuler as the protein marker, molecular weight of each band was labelled at left. Right lane: purified MT2a-FRET protein. The purity of the MT2a-FRET protein is > 90 %.

ATGGTGAAGAGCGAGGAGCTGTTACACGGGGTGGTGCCCATCCTGGTCGAGCTGGACGGGCGACGTAACGGCCACAGG
 M V S K G E E L F T G V V P I L V E D G D V N G H R
 TTCAGCGTGTCCGGCGAGGGCGATGCCACCTACGGCAAGCTGACCCCTGAAGTTCATCTGCACCACCGGCAAGCTG
 F S V S G E G E G D A T Y G K L T L K F I C T T G K L
 CCCGTGCCCTGGCCACCTCGTGACCACCTGACCTGGGGCGTGCAGTGTTCAGCCGCTACCCCGACCACTGAAGCAG
 P V P W P T L V T T L T W G V Q C F S R Y P D H M K Q
 CACGACTTCTTCAAGTCCGCCATGCCCGAAGGCTACGTCCAGGAGCGTACCATCTTCTTCAAGGACGACGGCAACTACAAG
 H D F F K S A M P E G Y V Q E R T I F F K D D G N Y K
 ACCCGCGCCGAGGTGAAGTTCGAGGGCGACACCTGGTGAACCCGCATCGAGTGAAGGGCATCGACTTCAAGGAGGACGGC
 T R A E V K F E G D T L V N R I E L K G I D F K E D G
 AACATCCTGGGGCACAAGCTGGAGTACAACCTACATCAGCCACAACGTCTATATCACCGCCGACAAGCAGAAGAAGGGCATC
 N I L G H K L E Y N Y I S H N V Y I T A D K Q K N G I Y
 AAGGCCCACTTCAAGATCCGCCACAACATCGAGGACGGCAGCGTGCAGCTCGCCGACCCTACCAGCAGAACACCCCCATC
 K A H F K I R H N I E D G S V Q L A D H Y Q Q N T P I
 GGCGACGGCCCCGTGCTGCCCGACACCACCTACCTGAGCACCCAGTCCGCCCTGAGCAAAGACCCCAACGAGAAGCGCC
 G D G P V L L P D N H Y L S T Q S A L S K D P N E K R
 GATCACATGGTCTGCTGGAGTTCGTGACCGCCGCCGCATGCATGATCCCAACTGCTCCTGCGCCCGGGTGACTCTGTC
 D H M V L L E F V T A A R M H D P N C S C A A G D S C
 ACCTGCGCCGCTCTGCAAAAGCAAAAGAGTCAAAAGTGCACCTCTGCAAGAAAAGCTGCTGCTCTGCTGCCCTGTGGGG
 T C A G S C K C K E C K C T S C K K S C C S C C P V G
 TGTGCCAAGTGTGCCAGGGCTGCATCTGCAAAGGGGGCTGGACAAGTGCAGCTGCTGCGCCGAGCTCATGGACGGCGGC
 C A K C A Q G C I C K G A S D K C S C C A E L M D G G
 GTGCAGCTCGCCGACCACTACCAGCAGAACACCCCATCGGGCGACGGCCCGTGTGCTGCTGCCGCAACCACTACCTGAGC
 V Q L A D H Y Q Q N T P I G D G P V L L P D N H Y L S
 TACCAGTCCGCCCTGAGCAAAGACCCCAACGAGAAGCGCGATCACATGGTCTGCTGGAGTTCGTGACCGCCGCGGGGATC
 Y Q S A L S K D P N E K R D H M V L L E F V T A A G I
 ACTCTCGGCATGGACGAGCTGTACAAGGGTGGCAGCGGTGGCATGGTGAAGGGGCGAGGAGCTGTTACCGGGGTGGTG
 T L G M D E L Y K G G S G G M V S K G E E L F T G V V
 CCCATCCTGGTCGAGCTGGACGGGCGACGTAACGGCCACAAGTTCAGCGTGTCCGGCGAGGGCGAGGGCGATGCCACCTAC
 P I L V E L D G D V N G H K F S V S G E G D A T Y
 GGCAAGCTGACCCCTGAAGCTGATCTGCACCACCGGCAAGCTGCCCTGCCCTGGCCACCCTCGTGACCACCTGGGCTAC
 G K L T L K L I C T T G K L P V P W P T L V T T L G Y
 GGCCTGCAGTGTTCGCCGCTACCCCGACCACTGAAGCAGCAGACTTCTTCAAGTCCGCCATGCCCGAAGGCTACGTC
 G L Q C F A R Y P D H M K Q H D F F K S A M P E G Y V
 CAGGAGCGACCATCTTCTTCAAGGACGACGGCAACTACAAGACCCGCGCCGAGGTGAAGTTCGAGGGCGACACCTGGTG
 Q E R T I F F K D D G N Y K T R A E V K F E G D T L V
 AACCGCATCGAGTGAAGGGCATCGACTTCAAGGAGGACGGCAACATCCTGGGGCACAAGCTGGAGTACAACCTACAACAGC
 N R I E L K G I D F K E D G N I L G H K L E Y N Y N S
 CACAACGTCTATATCACCGCCGACAAGCAGAAGAAGCGGCATCAAGGCCAAGCTTCAAGATCCGCCACAACATCGAGTAA
 H N V Y I T A D K Q K N G I K A N F K I R H N I E *

Figure S3. The complete DNA coding sequence and protein sequence of MT2a-FRET.

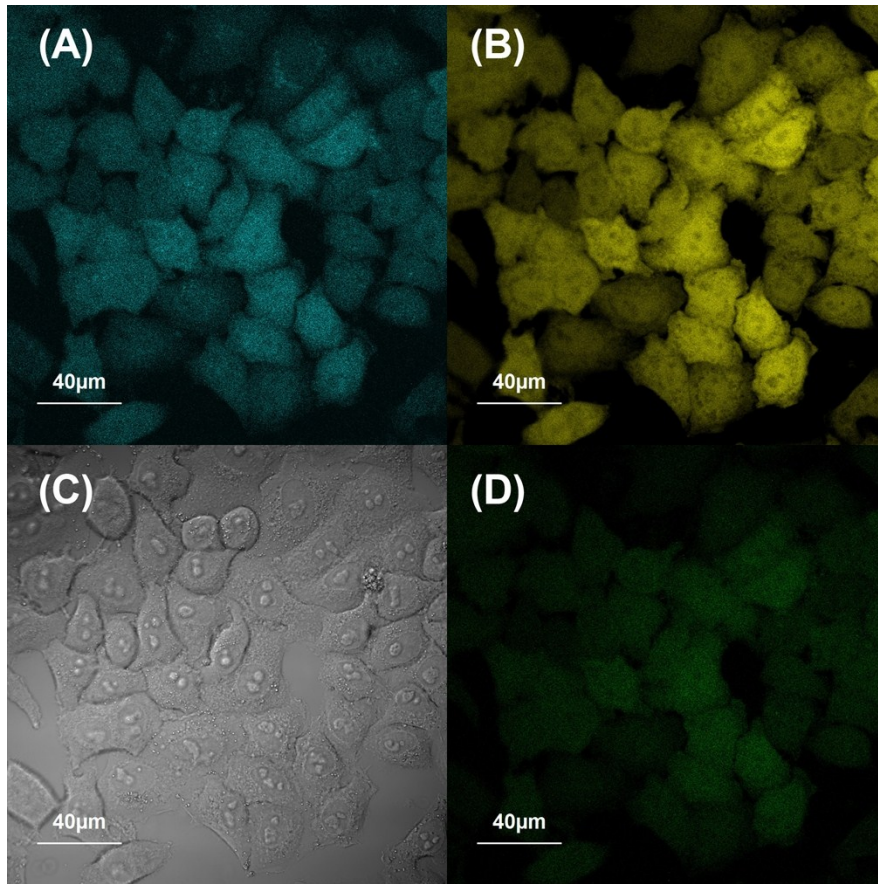


Figure S4. Images of the live MT2a-FRET cells under confocal microscope (Olympus FV1000 system). Images were taken with 60 × objective lens. (A) ECFP channel (Ex 405nm / Em 461 nm), (B) cpVenus channel (Ex 473nm / Em 527 nm), (C) Bright field channel and (D) FRET channel (Ex 405nm / Em 527 nm). Scale bar represents 40 μm.

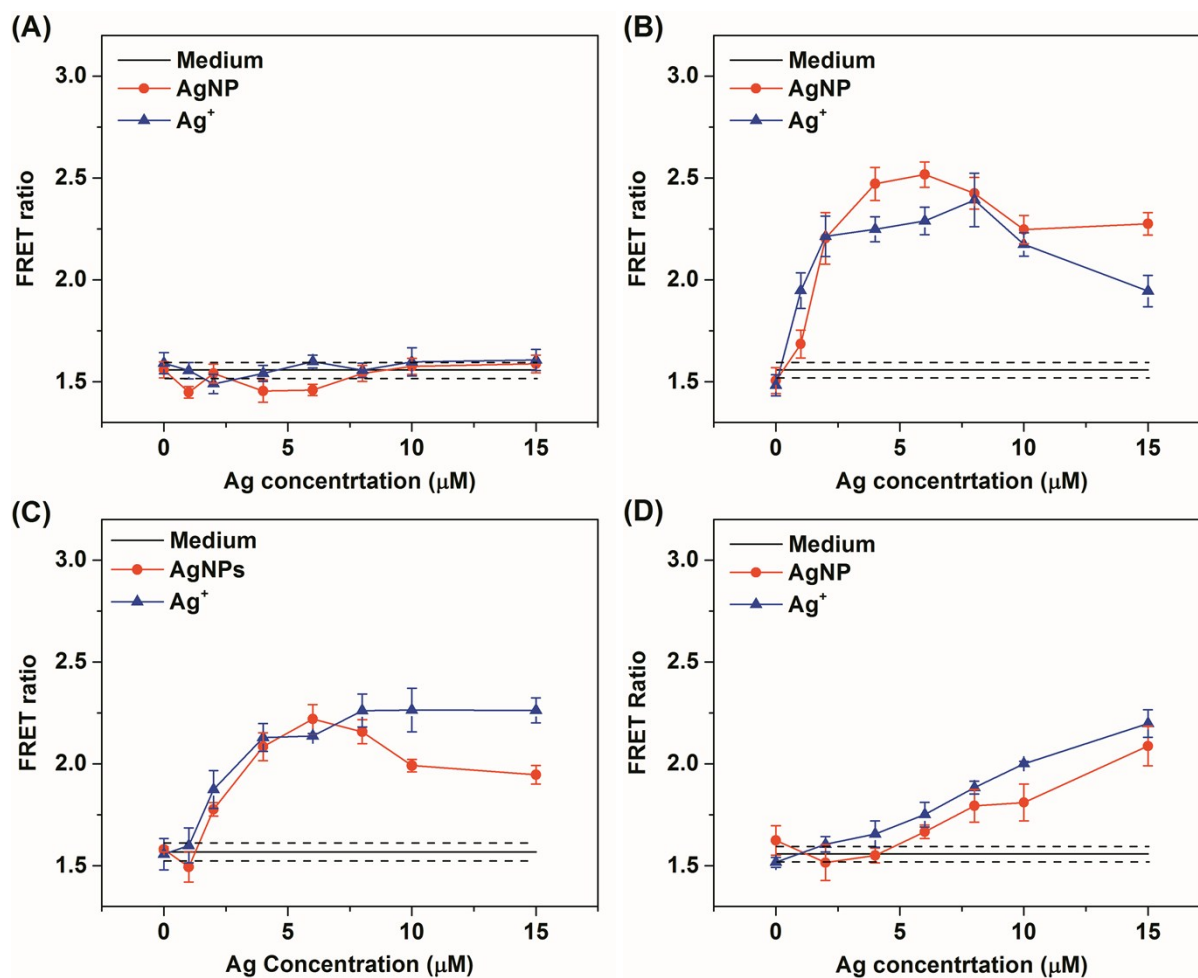


Figure S5. Comparisons of the FRET ratio in MT2a-FRET cells incubated with different atomic concentrations of AgNPs or AgNO₃ after (A) 0 h, (B) 6 h, (C) 24 h, and (D) 48 h treatment. The dashed lines represent the standard deviation of the medium group. The intracellular Ag⁺ gradually decreased to the same level for both AgNPs and AgNO₃ treatment, and the intracellular Ag⁺ were gradually diminished after 48 h treatment. Data are shown as mean ± SD (n=4).

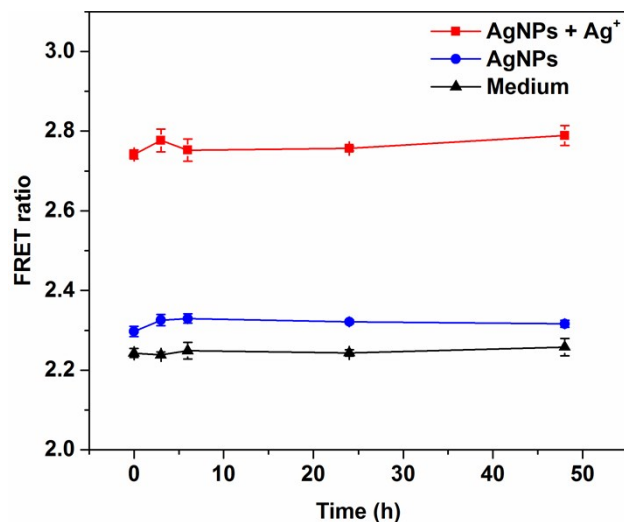


Figure S6. AgNP dissolution in cell culture medium. The cultured medium with 10 μM AgNPs from the cell FRET experiment was separated from the cells at different time point. Then 1 μM MT2a-FRET protein sensor was added to the cultured medium, and the FRET ratios were measured. After the measurement, additional 10 μM AgNO_3 was introduced to each well and the FRET ratios were measured again. The increase of the FRET ratios after AgNO_3 addition indicated that AgNPs in the cultured medium did not fully dissolved to Ag^+ . Data are shown as mean \pm SD (n=4).